

基于自适应滤波机理的脉冲激光近程探测 云雾干扰滤波方法

甘霖, 张合*

南京理工大学智能弹药技术国防重点学科实验室, 江苏 南京 210094

摘要 针对云雾环境对激光近程探测系统测距精度的影响, 提出了一种变步长自适应滤波方法。首先结合脉冲激光近程传输理论和 Mie 散射理论, 建立脉冲激光云雾传输后向散射模型, 在此基础上甄别、分离出云雾环境下脉冲激光回波的干扰信号; 然后根据干扰信号的特征, 采用自适应滤波方法滤除云雾干扰回波信号, 研究了云雾干扰下激光回波的脉宽、峰值和回波时刻这三种随机干扰因素对滤波性能的影响; 最后在实验室云雾环境下验证了所提滤波方法的效果。结果表明: 在不同的激光回波脉宽、功率以及回波时刻下, 所提自适应滤波方法具有良好的滤波效果和抗干扰性能, 能有效提高脉冲激光近程探测系统在云雾环境下的测距精度。

关键词 测量; 脉冲激光; 近程探测; 云雾干扰; 自适应滤波; 探测精度

中图分类号 TJ43 文献标志码 A

doi: 10.3788/CJL202249.0704001

1 引言

激光近程探测技术已被广泛应用于通信、航天、遥感和测距等领域^[1-4]。然而, 云雾干扰环境下的距离精确识别是激光近程探测的难点^[5-7]。脉冲激光的脉宽窄、峰值功率高、脉冲持续时间短, 而云雾粒子直径与脉冲激光波长尺寸接近, 极易产生以 Mie 散射现象为主的光学效应, 导致激光回波信号的幅值、脉宽等特征发生改变, 影响激光近程测距的精度^[8-9]。

针对云雾干扰对激光近程测距精度的影响, 美国尾刺和法国西北风导弹均采用紫外和红外双色制导体制, 通过目标与大气粒子对两种不同波长激光回波信号散射强度比值的差异来识别干扰。美国空对地激光雷达目标识别系统 ERAS-ER 采用载波调制技术来抑制云雾等模糊物的干扰^[10]。Rosprim 等^[11]和 Higuchi 等^[12]采用激光窄脉宽发射技术来降低粒子后向散射回波叠加效应以及减小回波干扰信号的功率。Heinonen^[13]用相邻距离信号相减来抑制云雾杂波干扰和识别真实目标, 并通过设置辅

助探测器来消除气溶胶粒子引起的虚警。法国 Thales 公司采用多扇形波束判别云雾干扰, 通过检测多个扇区回波信号的幅度变化率剔除了云雾干扰信号^[14]。上述多体制复合、多探测器辅助以及多波束探测的方法均采用了多个探测单元, 系统庞大且组成复杂, 而窄脉冲技术对系统功耗的要求非常严格, 因此, 上述方法难以解决小型激光近程探测系统云雾干扰的问题。

针对小型激光近程探测系统受云雾干扰的问题, 本课题组首先基于 Mie 散射理论建立了脉冲激光在云雾环境下传输的后向散射模型, 在此基础上分离提取出干扰回波信号; 之后, 针对干扰信号的特征, 提出了变步长自适应滤波方法, 用该方法抑制激光云雾回波信号对目标信号的干扰; 最后分析了激光云雾干扰信号的脉宽、峰值功率和出现时刻这三种随机因素对滤波效果的影响。

2 脉冲激光在云雾环境下近程探测时的后向散射干扰机理

脉冲激光的近程传输回波 $j(t)$ 可表示为

收稿日期: 2021-04-20; 修回日期: 2021-05-10; 录用日期: 2021-09-02

基金项目: 国家自然科学基金(51605227)、基础加强计划技术领域基金(2019-JCJQ-JJ-359)

通信作者: *hezhangz@mail.njust.edu.cn

$$j(t) = f(t) \otimes h(t), \quad (1)$$

式中: $f(t)$ 是激光发射波形; $h(t)$ 是脉冲冲击响应。采用重尾函数描述发射脉冲波形的时空分布,即

$$f(t) = (t/\tau)^2 \exp(-t/\tau), \quad (2)$$

式中: τ 表示激光发射脉宽; t 表示时间。 $h(t)$ 与目标的表面特性有关,可以表示为

$$h(t) = 4\pi\rho(\alpha)g(s)\delta(t - 2d/c), \quad (3)$$

式中: $\rho(\alpha)$ 表示目标表面的反射特性; $g(s)$ 为光强分布; d 是目标与测量系统的间距; $\delta(\cdot)$ 为狄拉克函数; c 代表光速。

采用双向反射函数(BRDF)来表述目标表面的反射特性^[15-16],即

$$\rho(\alpha) = \frac{A}{\cos^6 \alpha} \exp(-\tan^2 \alpha / \xi^2) + B \cos^m \alpha, \quad (4)$$

式中: A 、 B 分别表示镜面反射和漫反射的反射幅度; α 是入射角; ξ 被照射目标表面的斜率; m 是被照射目标表面的漫反射系数。光强分布采用高斯函数表示为^[17]

$$g(s) = \frac{2P}{\pi\omega_0^2 \left[1 + \left(\frac{\lambda d}{\pi\omega_0^2} \right)^2 \right]} \exp \left\{ \frac{-2s^2}{\pi\omega_0^2 \left[1 + \left(\frac{\lambda d}{\pi\omega_0^2} \right)^2 \right]} \right\}, \quad (5)$$

式中: P 是激光功率; ω_0 是光束束腰半径; λ 为激光波长; s 表示光束中心和横截面上点的距离。

云雾粒径分布采用 Gamma 分布表示^[8]

$$n(r) = ar^b \exp(-c'r^{d'}), \quad (6)$$

式中: $n(r)$ 为粒径分布函数; r 为粒子半径; a 、 b 、 c' 、 d' 为拟合参数。

基于 Lambert-Beer 定律,定义光子两次碰撞间的距离为散射自由程,其表达式为

$$\Delta s = -\frac{\ln \xi'}{\mu_t}, \quad (7)$$

式中: ξ 是在 $[0, 1]$ 上均匀分布的随机数; μ_t 为云雾衰减系数,其表达式为

$$\mu_t(\lambda) = \frac{3.912}{V} \cdot \left(\frac{\lambda}{0.55} \right)^{-q}, \quad (8)$$

式中: V 为能见度; q 为经验系数。根据 Naboulsi 等^[18]的研究结果,经验系数在近程范围内的数值为 0。

用散射相函数表征光子与云雾粒子碰撞后在各个方向上的散射强度。在非偏振状态下,散射相函数的表达式为^[19]

$$P(\theta) = \frac{|S_1(\theta)|^2 + |S_2(\theta)|^2}{\sum_{k=1}^{+\infty} (2k+1)(|a_k|^2 + |b_k|^2)}, \quad (9)$$

式中: a_k 、 b_k 为 Mie 散射系数; $S_1(\theta)$ 、 $S_2(\theta)$ 为散射振幅函数。

在上述脉冲激光近场探测回波模型的基础上,根据云雾模型和 Mie 散射理论,采用 Monte Carlo 方法模拟目标在云雾环境中的脉冲激光回波特性,步骤如下:

1) 根据初始参数(如表 1 所示),赋予光子初始运动方向和权重;

2) 当光子与云雾颗粒碰撞后,根据 Lambert-Beer 定律和散射相函数计算云雾散射脉冲激光的回波信息;

3) 当光子与目标接触后,根据目标反射特性对光子的运动方向和回波进行计算;

4) 将步骤 2) 和 3) 分别重复 100000 次,将云雾散射与目标部分回波叠加,获取云雾环境下脉冲激光的回波。

表 1 系统参数设置

Table 1 System parameter setting

System parameter	Value
Pulsed laser wavelength / nm	905
Launch system aperture / mm	10
Laser beam divergence / mrad	5
Receiving system aperture / mm	15
Receiving field angle / mrad	20
Laser transceiver spacing / mm	25
Peak photon number	100000
Cloud visibility / m	20
Target surface roughness	Diffuse reflection
Target distance / m	10

仿真回波信号如图 1 所示,当目标处于云雾环境中时,由于散射回波与目标回波时间间隔很短,两者会出现叠加,且回波信号会出现展宽等畸变,对脉冲激光测距精度造成了严重影响。同时,由于外界自然环境中云雾干扰等不确定性因素较多,干扰信号叠加强度及时刻具有很强的随机性,干扰信号的脉宽(PW)、峰值强度(PI)及其与目标回波的时间间隔 ΔT 等特征参数不能定量描述,上述随机干扰信号难以采用小波变换、高阶统计、经验模态分解(EMD)等方式进行滤波或屏蔽^[20-21]。

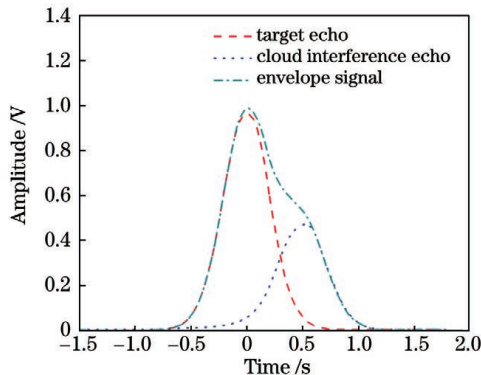


图 1 脉冲激光在云雾环境中的混合回波信号
Fig. 1 Mixed echo signal of pulsed laser in cloud environment

3 基于最小均方算法的云雾干扰信号自适应滤波方法

3.1 基于最小均方算法的云雾干扰滤波方法

自适应滤波算法已被广泛应用于信号识别、随机噪声消除等方面,最小均方(LMS)算法和递归最小二次方(RLS)算法是两种典型的自适应滤波算法。LMS算法基于误差均方最小原则滤除干扰信号,其算法和硬件简单,但收敛速度慢^[22];RLS算法基于加权误差平方和代价函数最小原则滤除干扰信号,收敛速度快,但算法和硬件组成复杂^[23]。考虑到激光探测的实时性以及系统体积与功耗的限制,本文基于LMS自适应滤波原理^[24-26]对激光回波云雾干扰进行自适应滤波。

自适应滤波器的一路输入是实际目标激光回波信号 $d(n)$ 与脉冲云雾干扰信号 $s(n)$ 的混合信号 $x(n)$,另一路输入是对云雾干扰信号的估计参考输入 $d(n)$,如图2所示。对输入 $x(n)$ 进行自适应滤波,使滤波器的输出 $y(n)$ 与 $d(n)$ 相匹配,则输出误差 $e(n)=\hat{s}(n)$ 即是对目标激光回波信号的最佳估计。

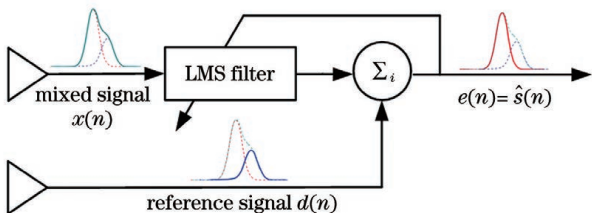


图 2 LMS 滤波原理
Fig. 2 LMS filtering principle

设混合信号 $x(n)$ 和参考信号 $d(n)$ 的长度为 N ,滤波器抽头数为 M ,令 n 的取值区间为 $[M, N]$,重复以下迭代过程

$$\mathbf{W}(n+1) = \mathbf{W}(n) + 2\mu \mathbf{X}(n) e(n), \quad (10)$$

式中: $\mathbf{X}(n)$ 为混合信号向量, $\mathbf{X}(n) = [x(n), x(n-1), \dots, x(n-M+1)]$; $\mathbf{W}(n) = \mathbf{0}$ 为滤波器抽头权向量; μ 为迭代步长因子; $e(n)$ 为误差, $e(n) = d(n) - y(n)$, $y(n) = \mathbf{W}^T(n) \mathbf{X}(n)$ 。通过误差 $e(n)$ 实时更新滤波器权向量,对混有复杂背景的信号实现自适应滤波。然而,传统LMS算法的收敛速度和稳态误差均依赖于迭代步长 μ ,因此,快速的收敛速度和较小的稳态误差难以同时满足^[25]。针对该问题,本文设计了一种滤除云雾环境下激光回波干扰信号特征且具有步长记忆效应的变步长算法。在该算法中,步长因子变为

$$\mu(n) = a_4 \mu(n-1) + a_5 p(n), \quad (11)$$

其中,

$$p(n) = a_3 \tanh[a_2 |e(n)|^{a_1}], \quad (12)$$

式中: $p(n)$ 为步长函数; $a_1 \sim a_5$ 为步长控制参数。首先讨论 $a_1 \sim a_3$ 的取值对步长因子的影响。 a_3 控制函数的取值范围,设定为0.5。在 $a_2=2, a_3=0.5, a_4=0.7, a_5=0.4$ 的条件下,当 a_1 分别取0.5、1、2、3、4时,步长函数 $p(n)$ 与误差函数 $e(n)$ 之间的关系如图3所示。可见, a_1 对 $p(n)$ 的收敛速度和底部形状有较大影响:当 $a_1=0.5$ 时,误差 $e(n)$ 在接近0时,即算法已达到或即将达到稳态时, $p(n)$ 急剧收敛,此时会造成较大的稳态误差;随着 a_1 增大,当误差 $e(n)$ 接近0时, $p(n)$ 的收敛速度越来越慢;当 $a_1=4$ 时,误差 $e(n)$ 还未接近0, $p(n)$ 就已为0,说明当误差 $e(n)$ 还在变化时, $p(n)$ 就已不再变化,此时会产生较大的稳态误差和稳态失调。综合分析收敛速度和算法复杂度可知:当 $a_1=2$ 时,在初始收敛阶段,较大的误差 $e(n)$ 产生了较大的 $p(n)$;进入稳态收敛阶段后,较小的误差 $e(n)$ 产生了较小的 $p(n)$ 。这一收敛特征有利于跟踪并减小稳态误差。

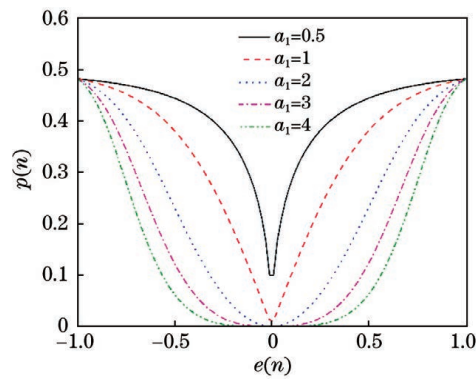


图 3 不同 a_1 下步长与误差之间的关系

Fig. 3 Relationship between step size and error in different a_1 values

在 $a_1=2, a_3=0.5, a_4=0.7, a_5=0.4$ 的条件下, 当 a_2 分别为 1、2、3、4、5 时, 步长函数 $p(n)$ 与误差函数 $e(n)$ 之间的关系如图 4 所示。可以看出, a_2 对 $p(n)$ 的收敛特征和函数形状有较大影响: 当 $a_2=1$ 时, 较大的误差 $e(n)$ 使得 $p(n)$ 快速变化, 不利于大步长跟踪较大的误差; 随着 a_2 增大, 在较大的误差范围内, $p(n)$ 的变化速度放缓, 此时有利于保持大步长跟踪较大的误差, 但随之而来的是在误差 $e(n)$ 接近 0 时, $p(n)$ 的收敛速度加快, 不利于小步长跟踪小误差。因此, 较小或较大的 a_2 都不利于步长实时跟踪变误差。在多次仿真分析和实验的基础上发现, 当 $a_2=3.4$ 时, $p(n)$ 会随着 $e(n)$ 的变化发生合理的改变, 有利于跟踪并降低误差。

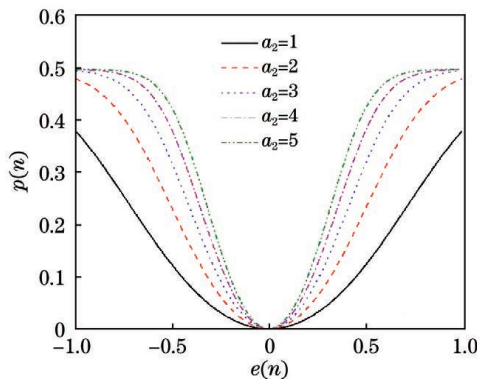


图 4 不同 a_2 下步长与误差之间的关系

Fig. 4 Relationship between step size and error in different a_2 values

在 $a_1=2, a_2=3.4, a_3=0.5, a_5=0.4$ 的条件下, 当 a_4 分别取 0.6、0.7、0.8、0.9 时, 算法的收敛性能表现出不同的特征。由图 5 可见, 随着 a_4 增大, 算法的收敛速度提高, 但收敛精度降低。如图 6 所示, 在 $a_1=2, a_2=3.4, a_3=0.5, a_4=0.8$ 的条件下, 当 a_5 分别取 0.3、0.4、0.5、0.6 时, 算法的收敛

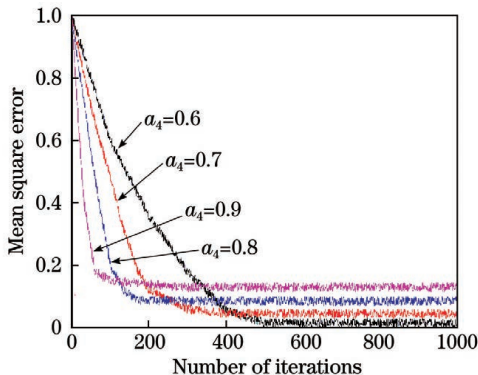


图 5 a_4 对算法收敛性能的影响

Fig. 5 Influence of a_4 on algorithm convergence performance

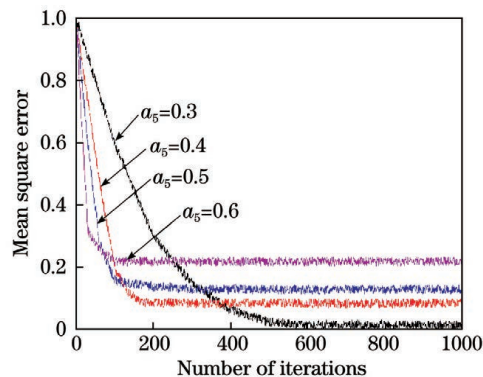


图 6 a_5 对算法收敛性能的影响

Fig. 6 Influence of a_5 on algorithm convergence performance

性能随 a_5 的变化表现出类似的规律。

通过上述分析可知, 取 $a_1=2, a_2=3.4, a_3=0.5, a_4=0.8, a_5=0.5$, 自适应滤波方法具有较好的滤波效果。

本课题组充分考虑了不同工况下的滤波效果, 针对不同的激光发射脉宽、云雾能见度、脉冲激光收发间距、探测装置与云雾以及目标的相对位置, 分别对应设置了云雾环境下不同的回波脉宽、回波幅值以及云雾干扰回波时刻, 并进行仿真分析。

3.2 云雾环境下激光回波信号脉宽对滤波效果的影响

首先分析云雾环境下不同脉宽的激光回波对滤波效果的影响。设定无云雾时激光回波信号幅值为 0.75 V, 脉宽为 5 ns, 云雾干扰信号幅值为 0.4 V, 脉宽分别为 5、10、15、20 ns, 云雾干扰信号波峰在无云雾环境激光回波信号波峰后 10 ns 出现, 模拟信号如图 7(a)所示。采用所提滤波方法处理后的激光回波信号如图 7(b)所示, 可见, 干扰信号幅值均被压缩至 0.056 V 左右, 激光回波脉宽扩展以及波峰效应减弱, 提高了信号还原度以及算法的处理精度。

3.3 云雾环境下激光回波信号能量对滤波效果的影响

不同的云雾能见度会导致干扰信号能量发生波动^[27-28], 下面讨论不同的干扰信号能量对滤波效果的影响。设定无云雾环境时的激光回波信号参数与上述一致, 云雾干扰信号脉宽为 15 ns, 幅值分别为 0.2、0.3、0.4、0.5 V, 云雾干扰信号波峰在无云雾环境下的激光回波信号波峰后 10 ns 出现, 模拟信号如图 8(a)所示。经所提滤波方法处理后的激光回波信号如图 8(b)所示, 可见, 经滤波后的干扰信号幅值随着原峰值的增加而增加(当原始输入峰值

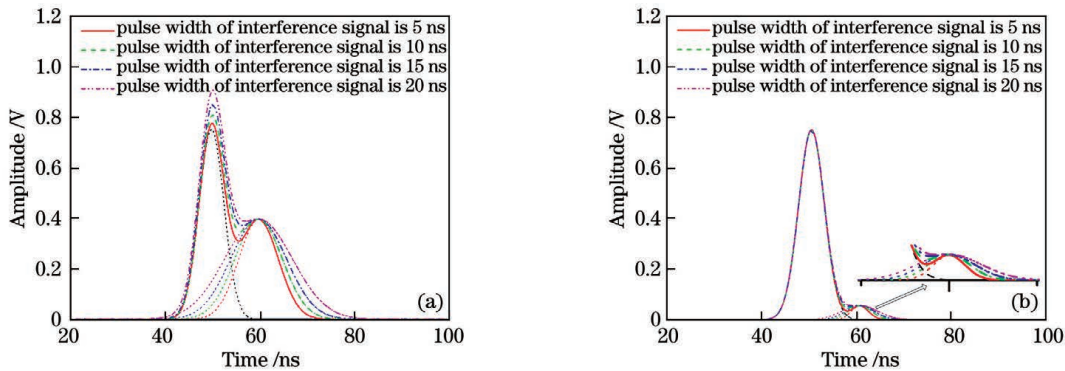


图7 云雾环境下不同脉宽激光回波干扰的仿真滤波对比。(a)原始干扰信号;(b)滤波后的信号

Fig. 7 Comparison of simulation filtering of laser echo interference with different pulse widths in cloud environment.

(a) Original interference signal; (b) filtered signal

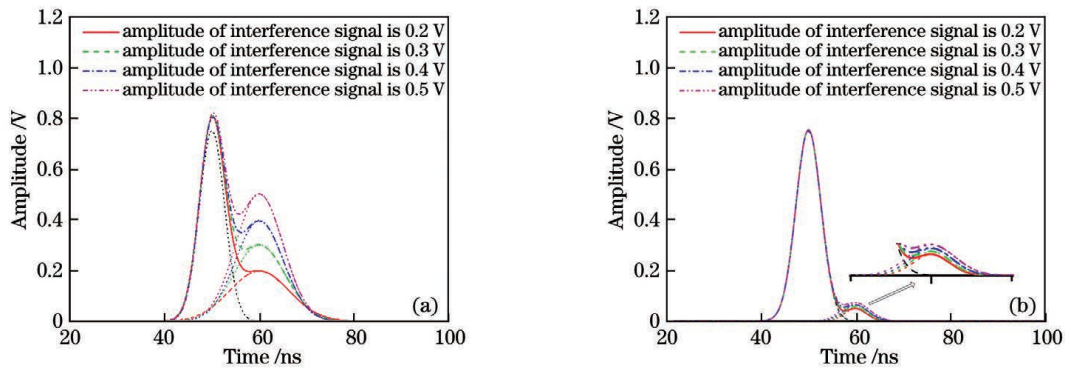


图8 云雾环境下不同能量激光回波干扰的仿真滤波对比。(a)原始干扰信号;(b)滤波后的信号

Fig. 8 Comparison of simulation filtering of laser echo interference with different energies in cloud environment.

(a) Original interference signal; (b) filtered signal

为0.5 V时,滤波后的峰值为0.072 V,当原始输入峰值为0.2 V时,滤波后的峰值为0.049 V),激光回波脉宽扩展以及波峰效应减缓。由此可见,本文提出的滤波方法可以有效滤除不同能量激光回波的云雾干扰信号。

3.4 云雾环境下激光回波信号出现时刻对滤波效果的影响

自然界中的云雾具有随机性,使得云雾干扰信

号出现时刻具有不确定性,因此,接下来考察不同云雾干扰信号出现时刻对本文滤波方法的影响。设定无云雾时的激光回波参数与上述一致,云雾干扰信号脉宽为15 ns,幅值为0.4 V,云雾干扰信号波峰分别在无云雾激光回波信号波峰前20 ns、10 ns以及波峰后10 ns、20 ns时出现,模拟信号如图9(a)所示。经本文滤波方法处理后的激光回波信号如图9(b)所示,结果显示:针对不同时刻的云雾干扰,

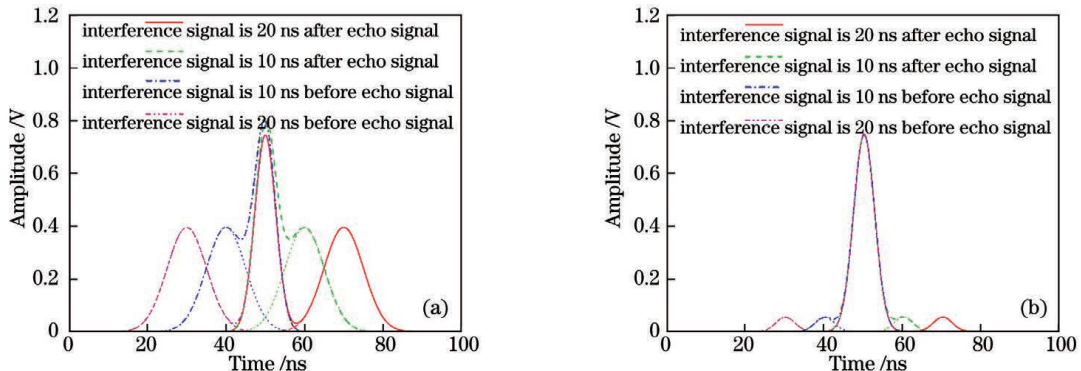


图9 云雾环境下不同时刻激光回波干扰的仿真滤波对比。(a)原始干扰信号;(b)滤波后的信号

Fig. 9 Comparison of simulation filtering of laser echo interference at different moments in cloud environment.

(a) Original interference signal; (b) filtered signal

干扰信号幅值均被抑制在 0.056 V 以下,包含云雾干扰信号的激光回波信号的有效部分与无云雾干扰时的激光回波信号相当。由此可见,本文提出的滤波方法可以有效降低不同时刻的云雾干扰信号。

4 实验验证

为了进一步验证本文所提滤波方法的实际性能,在云雾实验室搭建了脉冲激光近程探测系统;然后通过调整云雾浓度、目标距离和脉冲激光发射参数,获得了云雾干扰下不同的激光回波脉宽、功率及

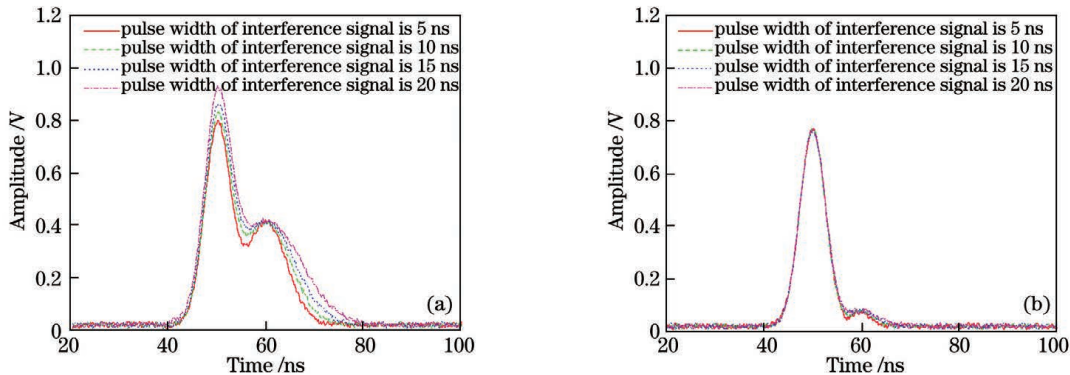


图 10 云雾环境下不同脉宽激光回波干扰的实验滤波对比。(a)原始干扰信号;(b)滤波后的干扰信号

Fig. 10 Comparison of experimental filtering of laser echo interference with different pulse widths in cloud environment.

(a) Original interference signal; (b) filtered signal

然后将入射能见度设置为 20 m, 调整目标距离, 当实际激光云雾回波干扰信号幅值分别为 0.2、0.3、0.4、0.5 V 时, 测试滤波后的信号, 测试

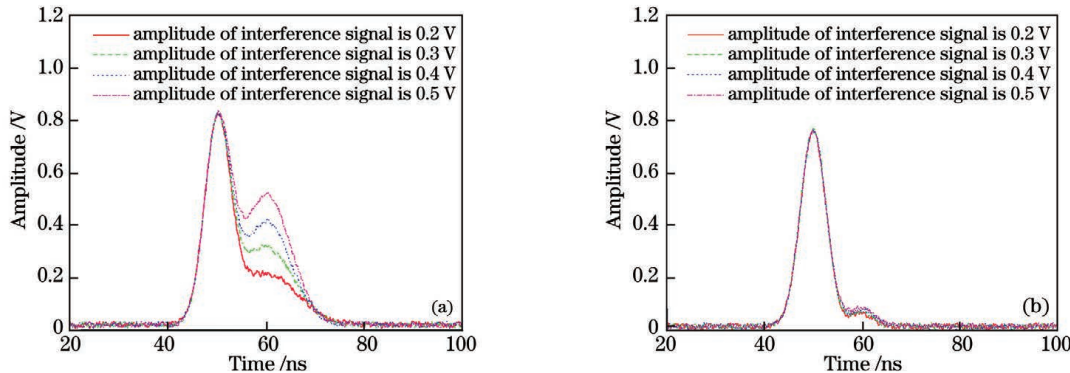


图 11 云雾环境下不同能量激光回波干扰的实验滤波对比。(a)原始干扰信号;(b)滤波后的信号

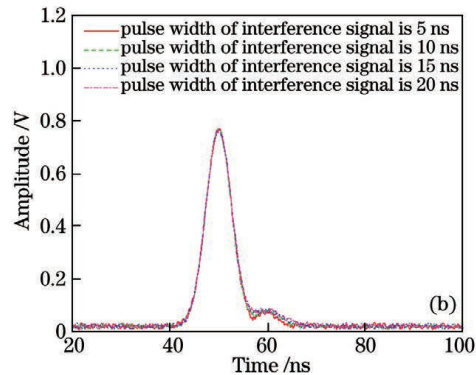
Fig. 11 Comparison of experimental filtering of laser echo interference with different energies in cloud environment.

(a) Original interference signal; (b) filtered signal

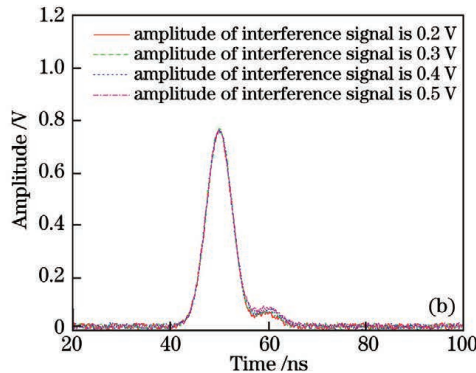
最后将入射能见度设置为 20 m, 调整目标和云雾团的相对位置, 当干扰信号分别在目标激光回波信号前 20 ns、10 ns 以及目标激光回波信号后 10 ns、20 ns 出现时, 测量实际激光云雾回波

回波时刻, 对比分析了不同状态下滤波前后的信号参数, 检验了滤波方法在实际云雾环境下的滤波效果。

首先将目标距离设置为 6 m, 入射能见度为 20 m, 调整脉冲激光发射参数, 将云雾干扰下的回波脉宽分别调整至 5、10、15、20 ns, 测量实际的云雾干扰激光回波信号以及经滤波处理后的干扰信号。测试结果如图 10 所示, 可见, 实际的云雾干扰激光回波信号的幅值在 0.4 V 左右, 经滤波处理后, 干扰信号幅值被压缩到 0.06 V 左右。



结果如图 11 所示。可见, 激光回波随机电磁干扰信号幅值分别被压缩到 0.055、0.0576、0.059、0.062 V。



信号和经滤波处理后的信号。测试结果如图 12 所示, 可见, 激光云雾回波干扰幅值在 0.4 V 左右, 滤波处理后信号幅值被压缩到 0.056 V 左右。

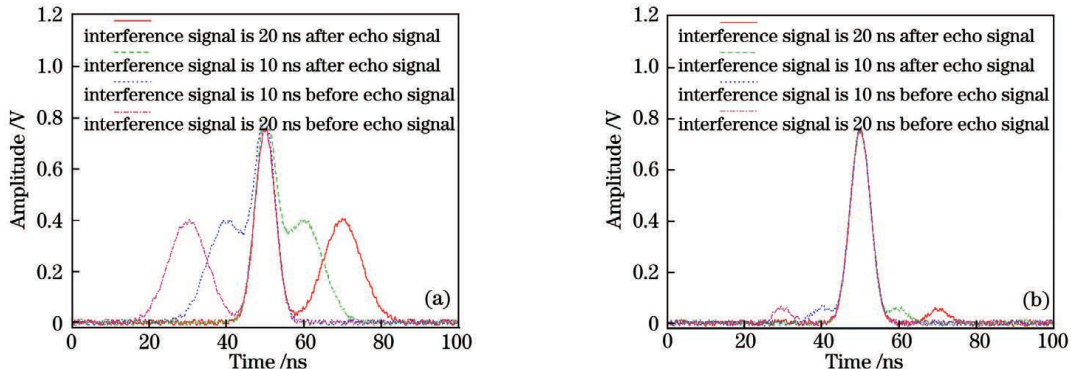


图 12 云雾环境下不同时刻激光回波干扰的实验滤波对比。(a)原始干扰信号;(b)滤波后的信号

Fig. 12 Comparison of experimental filtering of laser echo interference at different time in cloud environment.

(a) Original interference signal; (b) filtered signal

5 结 论

针对云雾环境对脉冲激光近程探测系统测距精度的影响,分析了激光云雾干扰回波信号的特征。基于LMS自适应滤波原理,设计了一种滤除激光云雾回波干扰信号特征且具有步长记忆效应的变步长滤波方法。为了验证该滤波方法的抗干扰性能,分别对激光云雾干扰回波脉宽、峰值功率和回波时间这三种随机干扰因素进行了分析。最后,进行了脉冲激光云雾环境干扰滤波对比实验,结果表明,本文所提自适应滤波方法可以有效滤除具有不同特征的云雾干扰信号,提高脉冲激光近程探测系统在云雾环境下的工作稳定性。

参 考 文 献

- [1] Xu J J, Bu L B, Liu J Q, et al. Airborne high-spectral-resolution lidar for atmospheric aerosol detection[J]. Chinese Journal of Lasers, 2020, 47(7): 0710003.
- [2] Walecki P, Taubin G. Super-resolution 3-D laser scanning based on interval arithmetic[J]. IEEE Transactions on Instrumentation and Measurement, 2020, 69(10): 8383-8392.
- [3] Nie S, Wang C, Xi X H, et al. Exploring the influence of various factors on slope estimation using large-footprint LiDAR data[J]. IEEE Transactions on Geoscience and Remote Sensing, 2018, 56(11): 6611-6621.
- [4] Quan Y, Li M Z, Zhen Z, et al. The feasibility of modelling the crown profile of larix olgensis using unmanned aerial vehicle laser scanning data [J]. Sensors, 2020, 20(19): 5555.
- [5] Li T, Chen S Y, Zhang Y C, et al. Simulation of water vapor multiple wavelengths lidar echo signals and error analysis[J]. Chinese Journal of Lasers, 2015, 42(2): 0213001.
- [6] Chen H M, Liu Y, Zhu X W, et al. Simulation of the characteristics of backscattering signals for frequency modulated continuous wave laser fuze[J]. Acta Armamentarii, 2015, 36(12): 2247-2253.
- [7] Chen P, Zhao J G, Song Y S, et al. Comparison on detection performance of FMCW and pulsed lidar in aerosol environment[J]. Infrared and Laser Engineering, 2020, 49(6): 20190399.
- [8] Wang F J, Chen H M. Simulation of characteristics of cloud and fog echo for pluse laser fuze [C] // Proceedings of 2015 Optical Precision Engineering Forum. Changchun: Editorial Department of Optics and Precision Engineering, 2015: 1-7.
- [9] Shishko V A, Konoshonkin A V, Kustova N V, et al. Light scattering by spherical particles for data interpretation of mobile lidars[J]. Optical Engineering, 2020, 59(8): 083103.
- [10] Chen P, Zhao J G, Song Y S. Research progress on anti-aerosol interference methods for laser proximity detection[J]. Journal of Ordnance Equipment

- Engineering, 2020, 41(8): 228-233.
- 陈鹏, 赵继广, 宋一铄. 激光近距探测抗气溶胶干扰方法研究进展[J]. 兵器装备工程学报, 2020, 41(8): 228-233.
- [11] Rosprim J P, Wang L, Podva D, et al. Progress in optimization of high-power high-speed VCSEL arrays [J]. Proceedings of SPIE, 2017, 10122: 1012205.
- [12] Higuchi A, Naito H, Torii K, et al. High power density vertical-cavity surface-emitting lasers with ion implanted isolated current aperture[J]. Optics Express, 2012, 20(4): 4206-4212.
- [13] Heinonen T. Planar imaging sensor having plural photo detector groups with different detection windows: US10209350[P]. 2019-02-19.
- [14] Chen P, Zhao J G, Song Y S, et al. Influence of microscopic characteristics of aerosol particles on backscattering echo[J]. Chinese Journal of Lasers, 2019, 46(4): 0405001.
陈鹏, 赵继广, 宋一铄, 等. 气溶胶粒子微观特性对后向散射回波的影响[J]. 中国激光, 2019, 46(4): 0405001.
- [15] Cai L, Zhang S Q, Guan X W. Theoretic analysis and experimental study on optical characteristics of extended targets[J]. High Power Laser and Particle Beams, 2013, 25(7): 1671-1674.
蔡雷, 张世强, 关小伟. 扩展目标光学特性的理论分析与研究[J]. 强激光与粒子束, 2013, 25(7): 1671-1674.
- [16] Han Y, Sun H Y, Guo H C. Analysis of influential factors on a space target's laser radar cross-section [J]. Optics & Laser Technology, 2014, 56: 151-157.
- [17] Jiang H J, Lai J C, Yan W, et al. Theoretical distribution of range data obtained by laser radar and its applications [J]. Optics & Laser Technology, 2013, 45: 278-284.
- [18] Naboulsi A M C, Sizun H, de Fornel F. Fog attenuation prediction for optical and infrared waves [J]. Optical Engineering, 2004, 43(2): 319-329.
- [19] Bohren C F, Huffman D R. Absorption and scattering of light by small particles[M]. Singapore: John Wiley & Sons, 1998.
- [20] Aggarwal R, Singh J K, Gupta V K, et al. Noise reduction of speech signal using wavelet transform with modified universal threshold [J]. International Journal of Computer Applications, 2011, 20(5): 14-19.
- [21] Inoue T, Saruwatari H, Takahashi Y, et al. Theoretical analysis of musical noise in generalized spectral subtraction based on higher order statistics [J]. IEEE Transactions on Audio, Speech, and Language Processing, 2011, 19(6): 1770-1779.
- [22] Huang F Y, Zhang J S, Zhang S. Mean-square-deviation analysis of probabilistic LMS algorithm[J]. Digital Signal Processing, 2019, 92: 26-35.
- [23] Jiang J, Vijayarajan V, Tan L Z. Channel sparsity aware function expansion filters using the RLS algorithm for nonlinear acoustic echo cancellation[J]. IEEE Access, 2020, 8: 118305-118314.
- [24] Kwong R H, Johnston E W. A variable step size LMS algorithm [J]. IEEE Transactions on Signal Processing, 1992, 40(7): 1633-1642.
- [25] Zhang Y. Adaptive algorithms and structures with potential application in reverberation time estimation in occupied rooms[M]. Cardiff: Cardiff University, 2007.
- [26] Schimmel G, Produtti T, Mongin D, et al. Free space laser telecommunication through fog [J]. Optica, 2018, 5(10): 1338-1341.
- [27] Li S L, Mao Z Y, Liu C H, et al. Analysis of the effect of cloud thickness on the performance of blue-green laser communication[J]. Opto-Electronic Engineering, 2020, 47(3): 190389.
- [28] Exertier P, Belli A, Samain E, et al. Time and laser ranging: a window of opportunity for geodesy, navigation, and metrology [J]. Journal of Geodesy, 2019, 93(11): 2389-2404.

Cloud Interference Filtering Method Based on Adaptive Filtering Mechanism for Pulsed Laser Short-Range Detection

Gan Lin, Zhang He^{*}

ZNDY of Ministerial Key Laboratory, Nanjing University of Science and Technology, Nanjing, Jiangsu 210094, China

Abstract

Objective Laser short-range detection technology has been widely used in communications, aerospace, remote sensing and ranging. However, the precise identification of distance in the environment of cloud and fog interference is a difficult problem for laser short-range detection. It is easy to produce optical effects dominated by Mie scattering due to the narrow pulse width, high peak power and short pulse duration of the pulsed laser; the diameter of the

cloud particles is close to the wavelength of the pulsed laser. This leads to changes in characteristics, such as the amplitude and pulse width of the laser echo signal, affecting the accuracy of laser short-range ranging. Because of the influence of cloud and fog interference on the accuracy of laser short-range ranging, several attempts have been made to adopt multi-system composites, multi-detector assistance and multi-beam detection methods. These methods use multiple detection units. The system is huge and complex; however, narrow pulse technology affects the system. Power consumption has strict requirements. Therefore, the above method cannot easily solve the problem of cloud and fog interference in a small laser short-range detection system.

Methods Aiming at the problem of cloud and fog interference in a small laser short-range detection system, a pulsed laser cloud and fog transmission backscatter model is established based on the Mie scattering theory, and the interference echo signal is separated and extracted. According to the characteristics of the interference signal, a variable step adaptive filtering algorithm is proposed to suppress the interference of laser cloud and fog echo signal to the target signal. The experiment analyses the influence of three random factors of different laser cloud interference signal pulse width, peak power and time of appearance on the filtering effect.

Results and Discussions When the target is in a cloud and fog environment, due to the short time interval between the scattered and target echoes, the two will overlap, and the echo signal will appear distorted, such as broadening; thus, severely impacting the accuracy of pulsed laser ranging. Since there are many uncertain factors in the interference of clouds and fog in the natural environment, the superimposed intensity of the interference signal and moment have strong randomness, and the pulse width (PW), peak intensity (PI) of the interference signal and the time interval between the interference signal and the target echo and other characteristic parameters cannot be described quantitatively. Additionally, it is not easy to filter or shield the above random interference signals by wavelet, high-order statistics and empirical mode decomposition (Fig. 1). The amplitude and pulse width are set as 0.75 V and 5 ns, respectively. The signal amplitude of the cloud interference part is set as 0.4 V and the pulse width is set as 5, 10, 15 and 20 ns, respectively. The peak of the cloud interference signal appears 10 ns behind the peak of the laser echo signal in the cloudless environment. The amplitude of the interference signal of the laser echo signal processed using the proposed filtering method is compressed to about 0.056 V. The PW of the laser echo is expanded, and the phenomenon of wave peak effect is weakened. Additionally, the signal reduction degree and algorithm processing accuracy are improved (Figs. 7 and 10). When the laser echo signal parameters are set in a cloudless environment, they are consistent with the above values. The PW of the cloud jamming signal is 15 ns; the amplitude is 0.2, 0.3, 0.4 and 0.5 V. The peak of the cloud jamming signal appears 10 ns after the peak of the laser echo signal in a cloudless environment. The amplitude of the laser echo signal processed using the proposed filtering method increases as the original peak value increases. When the original input peak value is 0.5 V, the filtered peak value is 0.072 V. In contrast, the filtered peak value is 0.049 V when the original input peak value is 0.2 V. The PW of the laser echo expands, and the phenomenon of wave peak effect slows down. The proposed filtering method can effectively target the laser echo cloud interference signals with different energies (Figs. 8 and 11). When the laser echo parameters are set as above, the PW and amplitude of the fog jamming signal are 15 ns and 0.4 V, respectively. The peak of the fog jamming signal appears at 20 ns, 10 ns before and 10 ns after the peak of the fog jamming signal. The amplitude of laser echo interference signals processed using the proposed filtering method is suppressed below 0.056 V. The effective part of the laser echo signal containing cloud interference signal is equivalent to the laser echo signal without cloud interference. Therefore, it can be seen that the proposed filtering algorithm can effectively reduce the laser cloud interference signal at different moments (Figs. 9 and 12).

Conclusions In view of the influence of cloud environment on the ranging accuracy of pulsed laser short-range detection system, the characteristics of laser cloud interference echo signal are analysed. A variable step-size filtering algorithm with step-size memory effect is proposed based on the principle of LMS adaptive filtering to characterise laser cloud echo interference signals. To verify the anti-jamming performance of the proposed filtering method, we analyse three factors of random jamming, pulse width, peak intensity, and echo time interval. A comparative experiment of pulsed laser cloud environment interference filtering is conducted. The results show that the proposed adaptive filtering algorithm can effectively target random parameter cloud interference signals and improve the working stability of pulsed laser short-range detection systems in a cloud environment.

Key words measurement; pulsed laser; short-range detection; cloud interference; adaptive filtering; detection accuracy